LETTERS
PUBLISHED ONLINE: 19 JUNE 2011 | DOI: 10.1038/NGEO1182
nature geoscience

Small temperature benefits provided by realistic afforestation efforts

Vivek K. Arora[1]* and Alvaro Montenegro[2]

Afforestation, the conversion of croplands or marginal lands into forests, results in the sequestration of carbon. As a result, afforestation is considered one of the key climate-change mitigation strategies available to governments by the United Nations[1]. However, forests are also less reflective than croplands, and the absorption of incoming solar radiation is greater over afforested areas. Afforestation can therefore result in net climate warming, particularly at high latitudes[2–5]. Here, we use a comprehensive Earth system model to assess the climate-change mitigation potential of five afforestation scenarios, with afforestation carried out gradually over a 50-year period. Complete (100%) and partial (50%) afforestation of the area occupied at present by crops leads to a reduced warming of around 0.45 and 0.25 °C respectively, during the period 2081–2100. Temperature benefits associated with more realistic global afforestation efforts, where less than 50% of cropland is converted, are expected to be even smaller, indicating that afforestation is not a substitute for reduced greenhouse-gas emissions. We also show that warming reductions per unit afforested area are around three times higher in the tropics than in the boreal and northern temperate regions, suggesting that avoided deforestation and continued afforestation in the tropics are effective forest-management strategies from a climate perspective.

We analyse simulations made with the first-generation Canadian Earth System Model[6,7] (CanESM1), which consists of coupled dynamical atmosphere and ocean models with full oceanic and terrestrial carbon-cycle components. This model reproduces twentieth-century observations of global mean atmospheric CO_2, as well as its seasonal cycle and interhemispheric gradient[6]. One standard simulation with no land-use/cover change (LUCC) and five afforestation simulations are carried out for the 2011–2100 period, all with emissions increasing according to the Special Report on Emissions Scenarios A2 scenario. These future simulations are continuations of an 1850–2010 historical simulation that is driven with observation-based fossil-fuel emissions and changes in crop area[8,9] (see Methods) and has simulated CO_2 concentration of 381 ppm in 2010. CO_2 is the longest-lived and most important of the major greenhouse gases and therefore we focus on the afforestation response to CO_2, which also simplifies the interpretation of our simulations.

Afforestation is carried out in areas that are at present occupied by croplands (Supplementary Fig. S1), and which, according to estimates of potential vegetation, would be occupied by forests if it were not for human activities (see Methods). The assumption is that afforestation is not a viable strategy if artificial supply of water or nutrients, or any other type of high-intensity management, is required. In the 100% global afforestation simulation, the fractional coverage of woody tree plant functional types (PFTs) is gradually increased, and the fractional coverage of crop PFTs is gradually decreased, from 2011 to 2060, until the crop area becomes zero by 2060. This unrealistic simulation provides an upper limit to potential climatic changes when the land cover is essentially returned to its preindustrial state. In the 50%-afforestation simulation only 50% of the global crop area in 2010 is afforested over the 2011–2060 period. This more realistic, but still somewhat extreme, scenario would require at least a doubling of crop yield to feed the human population as crop area is halved over time. The remaining three simulations are identical to the 50% global afforestation simulation but afforestation is carried out only over boreal (48.23° N–90° N), northern temperate (22.24° N–48.23° N) or tropical (18.58° S–22.24° N) latitudinal bands. The afforested areas in these simulations are summarized in Table 1. The prescribed changes in the fractional coverage of PFTs do not determine the structural attributes of vegetation, or carbon sequestered over land, which are dynamically determined as a function of simulated climate and atmospheric CO_2 concentration (see Methods). The changes to land cover in our simulations are less drastic than in earlier studies[3–5,10] and so provide insight into the effects of somewhat more realistic afforestation efforts in conjunction with continuous increase in emissions. In addition, afforestation is carried out gradually over the 2011–2060 (50 year) period rather than in a step change and its effects are inferred directly and not by inversion of results from deforestation simulations[10].

The simulated CO_2 concentration in the standard no-LUCC simulation increases from 381 ppm in 2010 to 760 ppm in 2100 (see Supplementary Fig. S2a). Afforestation leads to larger land carbon uptake and consequently lower atmospheric CO_2 concentration in all afforestation simulations compared with the standard no-LUCC case (Fig. 1a,b). The 100% and 50% global afforestation simulations yield 93 and 45 ppm lower CO_2 in 2100, respectively, than the standard no-LUCC simulation. The drawdown generated in northern-temperate- and tropical-afforestation (~20 ppm) simulations is more than double the drawdown produced by boreal afforestation (9 ppm). This is partly because the afforested area in the boreal simulation is about half that in the northern-temperate-afforestation simulation (Table 1). The tropical-afforestation simulation yields the same CO_2 drawdown as the northern-temperate-afforestation simulation despite its lower afforested area because carbon is sequestered at a faster rate per unit afforested area in the tropics than in temperate regions. Land carbon uptake increases by ~240 and ~120 Pg C in the 100% and 50% global afforestation simulations, respectively, compared with the no-afforestation case (Fig. 1a and Supplementary Fig. S2b). The 240 Pg C of land carbon uptake in the 100% afforestation

[1]Canadian Centre for Climate Modelling and Analysis, Environment Canada, PO Box 3065, STN CSC, University of Victoria, Victoria, British Columbia, V8W 3V6, Canada, [2]Environmental Sciences Research Centre, Department of Earth Sciences, St Francis Xavier University, Antigonish, Nova Scotia, B2G 2W5, Canada. *e-mail: vivek.arora@ec.gc.ca.

Table 1 | Global and land-only averaged temperature differences between the standard no-LUCC and the five cropland afforestation simulations for the 2081–2100 period.

	Simulation	Afforested area (million km^2)	Temperature difference compared with the no-afforestation case (°C)		Statistical significance
			Land only	Global	
1.	100% global afforestation	20.2	−0.63	−0.45	$p < 0.01$
2.	50% global afforestation	10.1	−0.31	−0.25	$p < 0.01$
3.	50% boreal afforestation	2.0	0.01	−0.04	$p > 0.25$
4.	50% northern temperate afforestation	4.7	−0.16	−0.11	$p > 0.05$
5.	50% tropical afforestation	2.7	−0.25	−0.16	$p < 0.01$

The statistical significance of global temperature differences is also shown on the basis of the unequal-variance Student *t*-test. Afforested areas in different simulations are also shown.

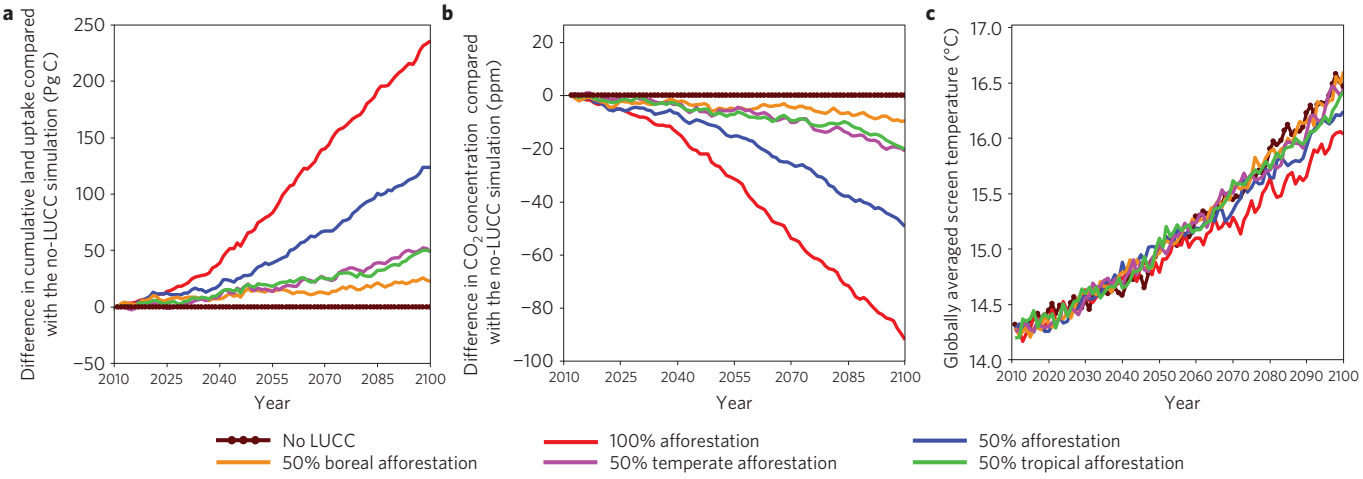

Figure 1 | Effect of cropland afforestation on land carbon uptake, atmospheric CO_2 and temperature. a,**b**, Differences in cumulative land uptake (**a**) and CO_2 concentrations (**b**) in the five afforestation simulations compared with the standard no-LUCC simulation. **c**, Simulated globally averaged screen temperature from all simulations.

simulation is larger than the 156 Pg C of cumulative land use change emissions over the 1850–2005 period[11] because the CO_2 fertilization effect results in more carbon sequestered per unit afforested area than there was in 1850. Ocean carbon uptake responds to atmospheric CO_2, with highest uptake in the no-LUCC simulation and lowest in the 100% afforestation case (Supplementary Fig. S2c).

All afforestation simulations yield lower temperatures (that is less warming) over the 2081–2100 period compared with the standard no-LUCC case, although the differences are not statistically significant ($p > 0.05$) for the northern-temperate- and boreal-afforestation simulations (see Fig. 1c and Table 1). Warming reductions are larger over land, except for the boreal afforestation, which yields a slight warming increase owing to the positive albedo effect[2]. Overall, the net temperature benefits of afforestation are small. Even the unfeasible scenario of afforesting all available cropland yields reduced warming of only 0.45 °C, with the still unrealistic 50% afforestation scenario resulting in a warming reduction of 0.25 °C over the 2081–2100 period, compared with 2.2 °C warming realized over the 2010–2100 period in the no-LUCC simulation (Fig. 1c). We define temperature effectiveness of afforestation (TEA), ξ, as

$$\xi = \frac{\Delta T}{A}$$

where ΔT (°C) is the globally averaged temperature difference averaged over the 2081–2100 period between an afforestation and the standard no-LUCC simulation and A (million km^2) is the area afforested. ΔT is used for the whole globe (ΔT_G) as well as only over land (ΔT_L) to obtain ξ_G and ξ_L shown in Fig. 2 for the five afforestation experiments. TEA values are negative, except for ξ_L for the 50%-boreal-afforestation experiment, because of the reduction in warming that afforestation yields. Quantified in this manner of reduced warming per unit afforested area, tropical afforestation is around three times more effective than afforestation in boreal and northern temperate regions.

The spatial patterns of the temperature response to afforestation are shown in Fig. 3. The 100%-afforestation simulation, in which all cropland area is afforested, leads to reduced warming almost everywhere except regions of high-latitude Eurasia (Fig. 3a). Here the regional enhanced warming associated with more radiation absorbed by the forests dominates the global reduction in warming associated with lower atmospheric CO_2. The magnitude of reduced warming is amplified in the Arctic because of the sea-ice albedo feedback. The northern high-latitude warming enhancement associated with lower albedo of forests is more widespread in the 50%-global-afforestation simulation (Fig. 3b) owing to its lower CO_2 drawdown, compared with the 100%-afforestation simulation. In the 50%-northern-temperate- and boreal-afforestation simulations warming enhancement is seen in northern mid/high-latitude regions, as expected, because the albedo effect of afforestation in these regions is strengthened by the presence of snow[2] (Supplementary Fig. S3a and S3b). These experiments also show areas of enhanced warming over parts of the Atlantic, Pacific and Southern

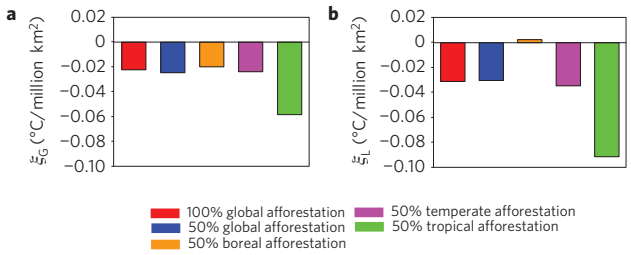

Figure 2 | Temperature effectiveness of afforestation (TEA). a,**b**, TEA values for the five afforestation experiments are calculated using temperature changes relative to the no-LUCC simulation and averaged over the 2081–2100 period over the whole globe (**a**) and over land only (**b**).

oceans. Tropical afforestation generally leads to widespread reduced warming but with enhancements over several oceanic regions (Supplementary Fig. S3c).

The United Nations Framework Convention on Climate Change (UNFCCC), through the Kyoto Protocol[12], enables the atmospheric carbon drawdown generated by afforestation to be accounted as sequestered carbon for the emission budget of the signatory nations. However, afforestation also changes the physical state of the land surface, which affects the regional and global energy balances. The effect of these radiative (related to surface albedo changes) and non-radiative (related to changes in evapotranspiration and surface roughness) biogeophysical changes are not easily obtained (see, for example, ref. 13) and therefore not at present taken into account by the UNFCCC. Here we decompose the reduced warming caused by afforestation into biogeophysical and biogeochemical components (see Methods) for the five afforestation simulations (Table 2), which interestingly add linearly to yield the net temperature response. Whereas the biogeochemical component yields reduced warming, relative to the no-LUCC simulation, owing to carbon sequestration associated with afforestation, the response to the biogeophysical changes in vegetation varies latitudinally, as is widely known[2,3] (Table 2). Biogeophysical changes associated with afforestation cause enhanced warming at mid–high latitudes associated with more absorption of incoming solar radiation and reduced warming in the tropics owing to higher evapotranspiration. The net result is that afforestation in the tropics provides double the benefits because both the biogeophysical and biogeochemical processes act to reduce warming. This is the reason why afforestation is around three times as effective in the tropics, in terms of reducing warming, as in northern temperate and boreal regions. Figure 3c–f shows the spatial pattern of the biogeophysical and biogeochemical components of the net temperature response to afforestation in the 100%- and 50%-afforestation simulations. As expected, the biogeophysical processes result in widespread enhanced warming, especially over northern mid/high-latitude land areas and in the Arctic region, where this warming is amplified owing to the sea-ice-albedo feedback. The effect of CO_2 drawdown in offsetting warming is nearly global in both simulations, with amplification in the Arctic region. In the 100%- and 50%-afforestation simulations the globally averaged biogeophysical component is near zero (Table 2 and Fig. 3c,d) and the net temperature response is almost solely determined by the biogeochemical component. This is an artefact of the enhanced biogeophysical warming at mid–high latitudes being compensated by reduced biogeophysical warming in the tropics, compared with the no-LUCC case.

Afforestation has been considered as a viable climate-change mitigation strategy. Our simulations suggest that, although this is true, the temperature benefits provided by afforestation are marginal. Afforesting 50% of the existing crop area, everywhere on the globe (an area much larger than the Amazon River basin), yields a warming reduction of 0.25 °C in the last two decades of the twenty-first century relative to the ∼3.0 °C temperature increase over the 1850–2100 period obtained using CanESM1 (for the A2 emission scenario). Temperature benefits of any realistic afforestation efforts, with afforested area less than that in the 50%-afforestation scenario, are expected to be even lower, suggesting that afforestation is not a substitute for reduced greenhouse-gas emissions. Moreover, in all afforestation simulations the temperature benefits are not realized until late in the twenty-first century. However, afforestation does provide several other benefits and ecosystem services, including wildlife habitat, provision of timber, pulp and paper, prevention of soil erosion and, through its sequestration of atmospheric CO_2, reduced acidification of the oceans. When interpreted on the basis of warming reduction per unit afforested area, the model simulations suggest avoided deforestation and continued afforestation in the tropics as more effective forest management strategies. Quantitative results presented here are subject to uncertainties, in particular those associated with the difference in the albedo of forests and croplands, climate sensitivity and the strength of the CO_2 fertilization effect, the latter two of which vary widely between models[14,15]. Biogeophysical and biogeochemical processes are influenced by all of these factors, so both the sign and magnitude of the net temperature response to afforestation are expected to vary between models. The climate sensitivity of CanESM1 is similar to that of most Coupled Climate Carbon Cycle Model Intercomparison Project models[16] (Supplementary Fig. S4) although its CO_2 fertilization effect is somewhat stronger[15]. Our finding, however, that the net temperature effect of any realistic afforestation efforts is an order of magnitude less than the warming realized over the 1850–2100 period is probably robust.

Methods

CanESM1 is a comprehensive coupled carbon–climate model[6,7] based on the third-generation atmospheric general circulation model of the Canadian Centre for Climate Modelling and Analysis, with horizontal resolution defined by a T47 triangular truncation for dynamical terms and ∼3.75° horizontal grid for physical terms. In the vertical, the model domain extends to 1 hPa atmospheric pressure with the thicknesses of the model's 32 layers increasing monotonically. The physical ocean component is based on the National Center for Atmospheric Research community ocean model with no flux adjustment. The ocean model is implemented at a horizontal resolution of ∼1.86° such that there are four ocean grid boxes underlying each atmosphere grid box. There are 29 levels in the vertical and the vertical resolution increases towards the ocean surface, from 300 m in the deep ocean to 50 m in the top 200 m. Atmospheric CO_2 is a fully prognostic three-dimensional tracer in CanESM1 and carbon enters and leaves the atmosphere in the form of anthropogenic emissions and fluxes to or from the underlying land and ocean. The biological and inorganic ocean carbon component of CanESM1 is the Canadian Model of Ocean Carbon, which incorporates an inorganic chemistry module (solubility pump) and an ecosystem model (organic and carbonate pumps)[17] based on a nutrient–phytoplankton–zooplankton–detritus model[18]. Terrestrial ecosystem processes in CanESM1 are modelled using the Canadian Terrestrial Ecosystem Model[6,19] for nine PFTs (needleleaf evergreen and deciduous trees, broadleaf evergreen and cold and drought deciduous trees, and C_3 and C_4 crops and grasses).

The historical simulation is carried out with prescribed fossil-fuel CO_2 emissions and land-use change up to 2010. Observation-based fossil-fuel CO_2 emissions[20] are used for the 1850–2000 period and emissions for the 2001–2010 period are based on the A2 scenario. The land cover is reconstructed using a historical crop-area data set[8] for the 1850–1992 period and its extension based on the A2 scenario for the 1993–2010 period[21,22]. Land-use-change emissions are calculated interactively in the model[9].

The preindustrial state of the land cover in 1850 is first used to generate a potential land-cover map[22]. Any grid-cell fraction occupied by crops in 1850 is substituted by non-crop PFTs in proportion to their fractional coverage within the grid cell at the time. This potential land-cover map, with no crop area, is then used as a guide to determine which of the five Canadian Terrestrial Ecosystem Model's tree PFTs are used to replace croplands when afforestation is implemented. An area is considered capable of being afforested if it is occupied by crops in 2010 and is, at the same time, occupied by tree PFTs in the potential land-cover map. Land surface

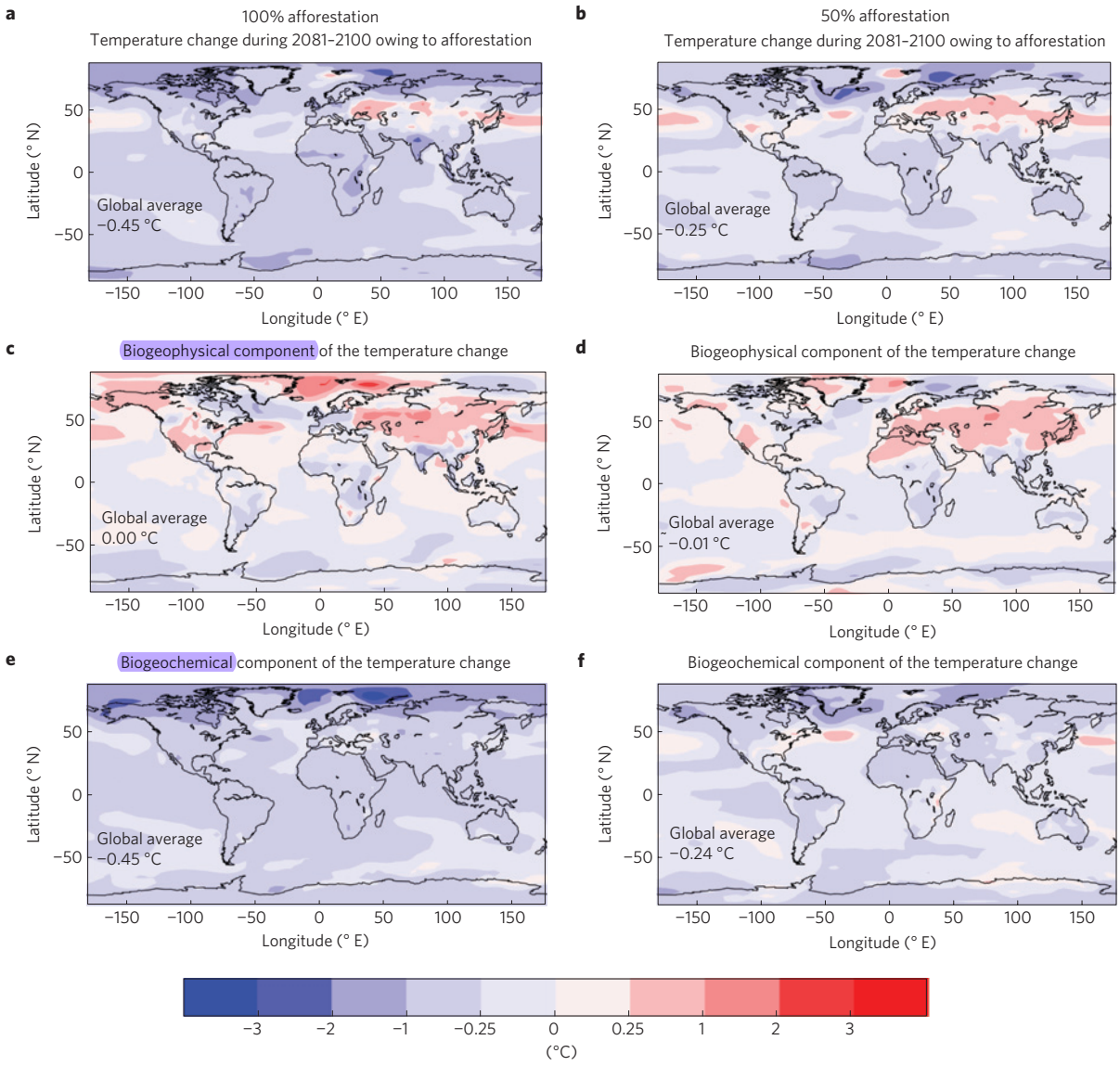

Figure 3 | Geographical pattern of temperature change owing to cropland afforestation and its separation into biogeophysical and biogeochemical components. a,**b**, Temperature change over the 2081–2100 period in the 100%- (**a**) and 50%- (**b**) afforestation simulations compared with the standard no-LUCC case. **c**–**f**, The biogeophysical component of this temperature change (**c**,**d**) and the biogeochemical component (**e**,**f**) for the 100%- and 50%-afforestation simulations, respectively. Negative values (blue colours) indicate reduced warming and positive values (red colours) indicate areas of enhanced warming.

Table 2 | Decomposition of the net globally averaged temperature response (°C) of afforestation over cropland area into biogeophysical and biogeochemical components.

	Simulation	Net temperature response	Biogeophysical component	Biogeochemical component
1.	100% global afforestation	−0.45	0.00	−0.45
2.	50% global afforestation	−0.25	−0.01	−0.24
3.	50% boreal afforestation	−0.04	0.01	−0.05
4.	50% northern temperate afforestation	−0.11	0.04	−0.15
5.	50% tropical afforestation	−0.16	−0.07	−0.09

albedo in CanESM1 depends on the albedo of vegetation, bare soil and snow (if present). A higher leaf area index of vegetation implies less visible bare-soil fraction and/or snow on the ground. As vegetation grows on the afforested fraction of grid cells the albedo changes rapidly (within ~5–7 years) owing to increases in leaf area index whereas carbon sequestration progresses slowly.

The decomposition of reduced warming, associated with afforestation, into biogeophysical and biogeochemical components is carried out using five further simulations, which use CO_2 concentration from the afforestation experiments but the changes in land cover associated with afforestation are not included (referred to as CO_2-only simulations). The difference between these CO_2-only and the corresponding afforestation simulations yields the biogeophysical component of the temperature effect of afforestation because they use the same CO_2 concentration but different land covers. Similarly, the difference between the standard no-LUCC and the corresponding CO_2-only simulations yields the biogeochemical component

of the temperature effect of afforestation (associated with CO_2 drawdown) because they use different CO_2 concentrations but the same land cover.

Received 17 January 2011; accepted 13 May 2011; published online 19 June 2011

References

1. Nabuurs, G. *et al.* in *IPCC Climate Change 2007: Mitigation. Contribution of Working Group III to the Fourth Assessment Report of the Intergovernmental Panel on Climate Change* (eds Metz, B., Davidson, O. R., Bosch, P. R., Dave, R. & Meyer, L. A.) (Cambridge Univ. Press, 2007).
2. Betts, R. A. Offset of the potential carbon sink from boreal forestation by decreases in surface albedo. *Nature* **408,** 187–190 (2000).
3. Gibbard, S., Caldeira, K., Bala, G., Phillips, T. J. & Wickett, M. Climate effects of global land cover change. *Geophys. Res. Lett.* **32,** L23705 (2005).
4. Schaeffer, M. *et al.* CO_2 and albedo climate impacts of extratropical carbon and biomass plantations. *Glob. Biogeochem. Cycles* **20,** GB2020 (2006).
5. Bala, G. *et al.* A. Combined climate and carbon-cycle effects of large-scale deforestation. *Proc. Natl Acad. Sci.* **104,** 6550–6555 (2007).
6. Arora, V. K. *et al.* The effect of terrestrial photosynthesis down-regulation on the 20th century carbon budget simulated with the CCCma Earth System Model. *J. Clim.* **22,** 6066–6088 (2009).
7. Christian, J. R. *et al.* The global carbon cycle in the CCCma earth system model CanESM1: Preindustrial control simulation. *J. Geophys. Res.* **115,** G03014 (2010).
8. Ramankutty, N. & Foley, J. A. Estimating historical changes in global land cover: Croplands from 1700 to 1992. *Glob. Biogeochem. Cycles* **13,** 997–1027 (1999).
9. Arora, V. K. & Boer, G. J. Uncertainties in the 20th century carbon budget associated with land use change. *Glob. Change Biol.* **16,** 3327–3348 (2010).
10. Claussen, M., Brovkin, V. & Ganopolski, A. Biogeophysical versus biogeochemical feedbacks of large-scale land cover change. *Geophys. Res. Lett.* **28,** 1011–1014 (2001).
11. Houghton, R. A. in *TRENDS: A Compendium of Data on Global Change* (Carbon Dioxide Information Analysis Center, Oak Ridge National Laboratory, US Department of Energy, 2008).
12. United Nations Framework Convention on Climate Change. *Decision 11/CP.7: Land Use, Land-use Change and Forestry*. Publication FCCC/CP/2001/13/Add.1 (2001).
13. Davin, E. L. & de Noblet-Ducoudre, N. Climatic impact of global-scale deforestation: Radiative versus nonradiative processes. *J. Clim.* **23,** 97–112 (2010).
14. Roe, G. H. & Baker, M. B. Why is climate sensitivity so unpredictable? *Science* **318,** 629–632 (2007).
15. Arora, V. K. & Matthews, H. D. Characterizing uncertainty in modeling primary terrestrial ecosystem processes. *Glob. Biogeochem. Cycles* **23,** GB2016 (2009).
16. Friedlingstein, P. *et al.* Climate–carbon cycle feedback analysis: Results from the C4MIP model intercomparison. *J. Clim.* **19,** 3337–3353 (2006).
17. Zahariev, K., Christian, J. R. & Denman, K. L. Preindustrial, historical, and fertilization simulations using a global ocean carbon model with new parameterizations of iron limitation, calcification, and N_2 fixation. *Prog. Oceanogr.* **77,** 56–82 (2008).
18. Denman, K. L. & Peña, M. A. A coupled 1-D biological/physical model of the northeast subarctic Pacific Ocean with iron limitation. *Deep-Sea Res. II* **46,** 2877–2908 (1999).
19. Arora, V. K. & Boer, G. J. A parameterization of leaf phenology for the terrestrial ecosystem component of climate models. *Glob. Change Biol.* **11,** 39–59 (2005).
20. Marland, G., Boden, T. A. & Andres, R. J. *Trends: A Compendium of Data on Global Change.* (Carbon Dioxide Information Analysis Center, Oak Ridge National Laboratory, 2008).
21. Alcamo, J., Leemans, R. & Kreileman, E. *Global Change Scenarios of the 21st Century: Results From the IMAGE 2.1 Model* (Elsevier, 1998).
22. Wang, A., Price, D. & Arora, V. Estimating changes in global vegetation cover (1850–2100) for use in climate models. *Glob. Biogeochem. Cycles* **20,** GB3028 (2006).

Acknowledgements

We would like to thank G. Flato, J. Fyfe and D. Blain and the two anonymous reviewers for their helpful comments. A.M. is grateful for funding from the Natural Sciences and Engineering Research Council. We also acknowledge the work of Canadian Centre for Climate Modelling and Analysis members who developed CanESM1 including, as well as the first author, G. J. Boer, C. L. Curry, J. R. Christian, K. Zahariev, K. L. Denman, G. M. Flato, J. F. Scinocca, W. J. Merryfield, W. G. Lee and D. Yang for help with processing model output.

Author contributions

V.K.A. carried out the model simulations, analysed model output, conceived the CO_2-only experiments and wrote most of the paper. A.M. conceived the primary experiments, put together land-cover data and helped with the manuscript text.

Additional information

The authors declare no competing financial interests. Supplementary information accompanies this paper on www.nature.com/naturegeoscience. Reprints and permissions information is available online at http://www.nature.com/reprints. Correspondence and requests for materials should be addressed to V.K.A.